Journal of Medicinal Chemistry

pubs.acs.org/jmc

Drug Annotation

CC-90009: A Cereblon E3 Ligase Modulating Drug That Promotes Selective Degradation of GSPT1 for the Treatment of Acute Myeloid Leukemia

Joshua D. Hansen,* Matthew Correa, Matt Alexander, Mark Nagy, Dehua Huang, John Sapienza, Gang Lu, Laurie A. LeBrun, Brian E. Cathers, Weihong Zhang, Yang Tang, Massimo Ammirante, Rama K. Narla, Joseph R. Piccotti, Michael Pourdehnad, and Antonia Lopez-Girona

Cite This: *J. Med. Chem.* 2021, 64, 1835−1843

Read Online

ACCESS | Metrics & More | Article Recommendations | Supporting Information

ABSTRACT: Acute myeloid leukemia (AML) is marked by significant unmet clinical need due to both poor survival and high relapse rates where long-term disease control for most patients with relapsed or refractory AML remain dismal. Inspired to bring novel therapeutic options to these patients, we envisioned protein degradation as a potential therapeutic approach for the treatment of AML. Following this course, we discovered and pioneered a novel mechanism of action which culminated in the discovery of CC-90009. CC-90009 represents a novel protein degrader and the first cereblon E3 ligase modulating drug to enter clinical development that specifically targets GSPT1 (G1 to S phase transition 1) for proteasomal degradation. This manuscript briefly summarizes the mechanism of action, scientific rationale, medicinal chemistry, pharmacokinetic properties, and efficacy data for CC-90009, which is currently in phase 1 clinical development.

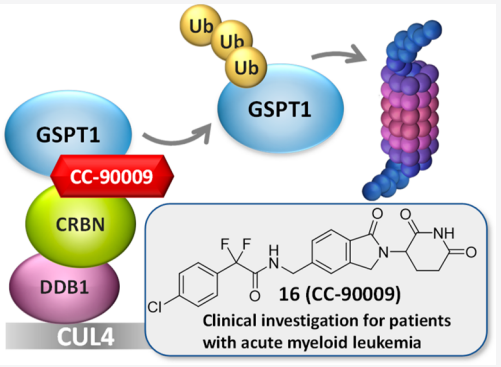

INTRODUCTION

CC-90009 2-(4-chlorophenyl)-*N*-((2-(2,6-dioxopiperidin-3-yl)-1-oxoisoindolin-5-yl)methyl)-2,2-difluoroacetamide, is a cereblon E3 ligase modulating drug (CELMoD) with antiproliferative and proapoptotic activity against acute myeloid leukemia (AML). CC-90009 derives its anti-AML efficacy through degradation of GSPT1 (G1 to S phase transition 1) and is currently in phase 1 clinical trials for relapsed/refractory acute myeloid leukemia.

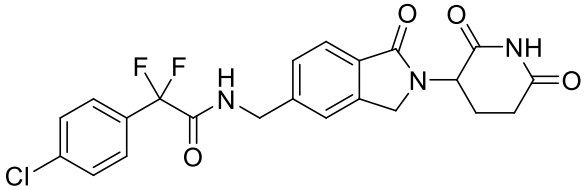

Acute myeloid leukemia is a relatively rare malignancy (~20 000 estimated diagnoses domestically in 2020) and is considered an orphan disease by the US Food and Drug Administration.[1,2] Despite advances in understanding the pathogenesis of AML, there remains significant clinical need due to both poor survival and high relapse rates in AML where the standard of care for fit patients is conventional intensive cytotoxic chemotherapy. 7+3 chemotherapy (7 days of cytarabine and 3 days of daunorubicin) and hematopoietic stem cell transplantation (HSCT) form the mainstay of induction/consolidation treatment, resulting in 5-year overall survival (OS) of 40% for patients younger than 60 years. AML, however, is mostly a disease of older individuals with a median age at diagnosis of 68. Of those who are 65 years or older, up to 70% will not survive beyond 1 year.[3] The recent FDA approval of the combination therapy venetoclax plus azacitidine has established a new standard of care for older patients with newly diagnosed AML by demonstrating a median overall survival of 14.7 months. This approval also provides an opportunity to combine with additional novel agents to improve the survival benefit further.[4] Nonetheless, for patients who are refractory or relapse from frontline therapy, the prognosis remains dire.

Protein Degradation. Targeted protein degradation represents a new paradigm in drug discovery, in which small molecules can be used to induce novel protein−protein interactions and enable destruction of target proteins that drive disease. Under the canopy of protein degradation, multiple modes of interaction have been reviewed that induce protein−

Received: August 26, 2020
Published: February 16, 2021

https://dx.doi.org/10.1021/acs.jmedchem.0c01489
J. Med. Chem. 2021, 64, 1835−1843

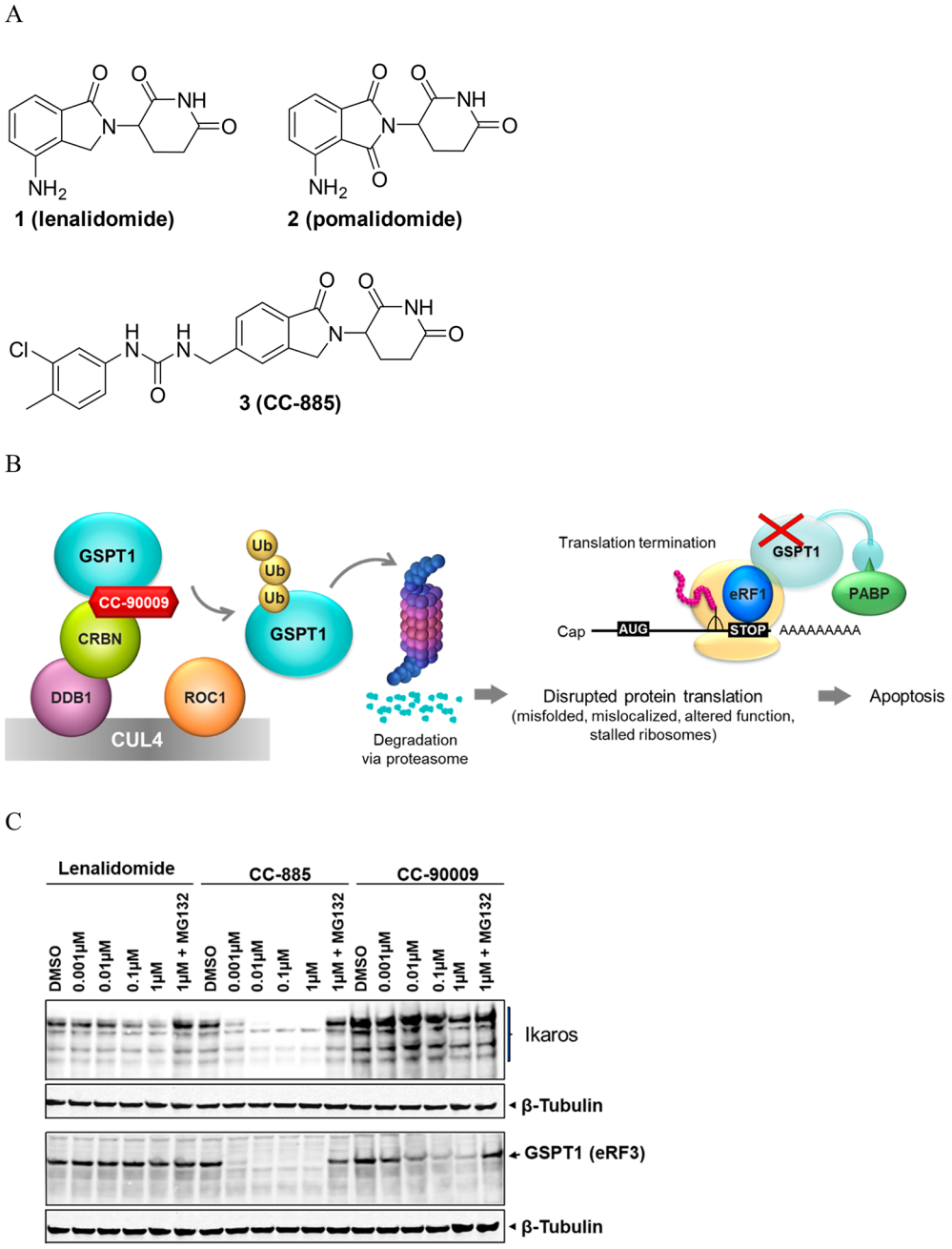

Figure 1. (A) Structures of lenalidomide, pomalidomide, and CC-885. (B) Proposed mechanism of action for CC-90009. (C) NB4 cells were treated for 4 h and then processed for Western blotting. CC-90009 selectively degrades GSPT1 (lenalidomide and CC-885 shown for comparison), which can be rescued with cotreatment of proteasome inhibitor MG132.

protein proximity,[5] and more specifically, two modes of degraders known as heterobifunctional degraders (PROTACs)[6,7] and molecular glues (CELMoDs)[7] have been reviewed. Both PROTACs[8] and CELMoDs[9] use protein degradation mechanisms characterized with recent advancement of small molecule degraders into clinical phase investigation.

Induction of protein degradation as a therapeutic strategy has been clinically validated by the class of immunomodulatory drugs developed by Celgene which include lenalidomide and pomalidomide (Figure 1A). Removal of disease-driving proteins translates to the therapeutic benefits derived from immunomodulatory drug treatment. Specifically, CELMoDs (including immunomodulatory drugs) have the capacity to induce recruitment followed by ubiquitination of substrate proteins to the $CRL4^{CRBN}$ E3 ubiquitin ligase, after which, ubiquitin tagged proteins are trafficked to and subsequently degraded by the 26S proteasome.[10−12] Small molecules utilized for this purpose are commonly referred to as "molecular glues" for their ability to draw two unrelated proteins together through ternary complex formation. This interaction between the two unrelated proteins achieved through ternary complex formation, does not occur in the absence of "molecular glue".

While lenalidomide and pomalidomide are known to derive efficacy in multiple myeloma via degradation of the transcription factors IKZF1/3,[12] CC-90009 is a novel molecular glue that directs an alternative degradation profile in which IKZF1/3 are spared and, instead, GSPT1/eRF3a (G1 to S

https://dx.doi.org/10.1021/acs.jmedchem.0c01489
J. Med. Chem. 2021, 64, 1835−1843

phase transition 1/eukaryotic Release Factor 3a) is degraded (Figure 1B and C).

RESULTS AND DISCUSSION

Focused on employing protein degradation as a strategy to address high unmet medical need, our goal was to discover a novel CELMoD that demonstrated improved clinical efficacy and an expanded treatment scope in AML which would potentially benefit patients across all age stratifications. To widen the possibilities of finding novel proteins that when degraded cause anti-AML activity, we envisioned that a phenotypic screen of our cereblon (CRBN) modulator library would be an expedient approach. Using this type of unbiased approach could afford potential to address an incomplete understanding and complexity found with AML, and in parallel, uncover novel biology not yet linked to AML with a first in class opportunity. It should be noted that there are disadvantages when employing phenotypic screening such as hit validation and target deconvolution.[13] However, in our case, the latter could be addressed by interrogating a focused library of CRBN-interacting chemical matter. In this manner, by using a phenotypic screen with CRBN-directed chemical matter, we already knew "half the target" (CRBN). Once shown to be CRBN-dependent, we could unravel the ubiquitylated target protein via pull down or by proteome analysis.

Because AML is characterized by high heterogeneity and coupled with our desire to broadly transform the disease landscape, we selected a panel of cell lines designed to represent many known genetic mutations to screen our CELMoD compound library for breadth of activity and develop SAR (Table 1). Using this panel of AML cell lines for the phenotypic screen rather than rely on a single cell line was also part of the strategy to evaluate activity trends holistically, and allowed incorporating activity breadth (in AML cell lines) versus toxicity as a profile of interest.

Table 1. Panel of AML Cell Lines and Associated Characterization[a]

cell line	genetic traits	AML FAB classification
KG-1	FGFR1 Act; NRas	FAB M0/1
HL60	$Myc^{amplified}$	FAB M2
NB4	Pml-Rara	FAB M3
KG-1a	FGFR1 act NRas	FAB M0/1
Kasumi-1	RUNX1-RUNX1T1; $KIT^{N822\ K}$	FAB M2
MV4-11	Mll-Af4; $FLT3^{ITD}$	FAB M5
OCI-AML-2	$DNMT3A^{R635W}$	FAB M4
U937	CALM-AF10	FAB M5
MOLM13	Mll-Af9; $FLT3^{ITD}$	FAB M5a
OCI-AML3	NPM1c; $DNMT3A^{R882C}$	FAB M4

[a]FAB stands for French-American-British and is a classification of AML into subtypes M0 to M7 based on cell origin and maturity.[14]

Structure–Activity Relationships (SAR). Recently, we described the SAR of a series of urea containing compounds represented by **3** (Figure 1A) which were observed to degrade the proteins Aiolos (IKZF3), Ikaros (IKZF1), and GSPT1 (eRF3a) with variable levels of selectivity.[15] Compound **3** displayed potent and broad activity against the AML cell line panel utilized for our phenotypic screen. However, compound **3** was considered unsuitable for further development due to concerns about its potential toxicity profile as a result of indiscriminate cell killing. This is highlighted by its cytotoxic activity against the nontumor human epithelial cell line (THLE-2), a line that can help prioritize compounds for having lower probability of causing adverse events in vivo[16] (Table 2).

Table 2. Comparison of the Antiproliferative Potency for CC-885 against a Panel of AML Cell Lines and THLE-2

cell line	CC-885 IC_{50} (μM)
KG-1	0.007
HL-60	0.003
KG-1a	0.008
KASMUI	0.010
NB4	0.002
MV-4-11	0.005
MOLM-13	0.008
OCI-AML2	0.021
OCI-AML-3	0.073
U-937	0.011
THLE-2	**0.011**

Because **3** did show potent and broad activity against the AML cell line panel, it provided a structural template for us to explore the possibility of identifying analogues with increased therapeutic index. To achieve this aim, we explored SAR of the chemical template and monitored the in vitro selectivity ratio between the various AML cell lines contained within our phenotypic panel and the THLE-2 line. The KG-1 cell line is highlighted in this manuscript as a representative example to demonstrate SAR in the series. A thorough investigation to optimize or replace the terminal 3-Cl, 4-Me aryl group was made but without improvement of the in vitro selectivity ratio. Additionally, attempts were made to substitute at either urea-nitrogen which also failed to yield improved in vitro selectivity windows, and this approach was ultimately abandoned.[15] Continued empirical modifications led us to discover that the most relevant impact on selectivity vs THLE-2 cells was made via SAR investigations around the urea linker. To set a baseline for comparison with the urea functionality, we utilized a derivative of **3**, the unsubstituted phenyl urea **4** which, like **3**, also exhibited a low in vitro selectivity ratio when comparison was drawn between KG-1 and THLE-2 cells (Table 3).

Table 3. SAR Comparison of the Antiproliferative Potency against AML Cell Line KG-1 and THLE-2

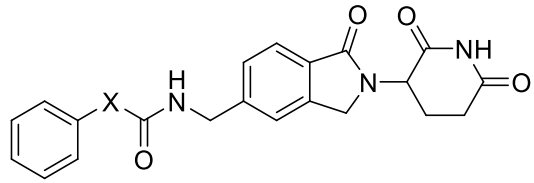

analogue	X	KG-1 IC_{50} (μM)	THLE-2 IC_{50} (μM)	in vitro selectivity ratio
4	X = NH	0.015	0.060	4×
5	X = CH_2	0.037	0.231	6×
6	X = none (benzamide)	>10	>10	
7	X = CO	0.009	0.196	22×
8	X = $C(CH_3)_2$	>10	>10	
9	X = CF_2	0.097	>10	**>100×**

https://dx.doi.org/10.1021/acs.jmedchem.0c01489
J. Med. Chem. 2021, 64, 1835−1843

Removal of the distal nitrogen atom and replacement with carbon led to amide **5**, which had little impact on the selectivity ratio. Truncation of the structure by deletion of the distal urea nitrogen atom provided benzamide **6** which was inactive. Comparison of the phenylacetamide functionality in **5** to the oxo acetamide contained in **7** gave us the first hint that selectivity between tumor and normal cell lines could be tempered. Although a THLE-2 IC_{50} of 196 nM was still concerning, compound **7** did maintain single digit nanomolar activity against KG-1 with a 22× selectivity window against THLE-2. The SAR in this region was found to be highly sensitive as dimethyl substitution on the phenyl acetamide carbon was not tolerated (**8** versus **5**). However, we were pleased to discover that the smaller difluoro substituent in compound **9** maintained activity below 100 nM against KG-1 cells, and importantly, an IC_{50} > 10 μM was observed in THLE-2 cells. This difluoro substitution pattern yielded an in vitro selectivity ratio >100× (KG-1 vs THLE-2 potency) which provided impetus to further optimize this difluoro acetamide series and ultimately led to the selection of CC-90009 as a clinical candidate.

In Vitro Pharmacology. To show that CC-90009-induced loss of GSPT1 was mediated via proteasomal degradation, KG-1 cells were treated with drug, which showed GSPT1 degradation by Western blot. When the KG-1 cells were cotreated with drug plus the proteasome inhibitor bortezomib or the neddylation inhibitor MLN4924, rescue of GSPT1 degradation was observed (Figure 2A). Loss of GSPT1 in leukemic cells leads to activation of the integrated stress response (ISR), which is an evolutionarily conserved homeostatic pathway. ISR pathway activation results in the inhibition of global protein translation and preferential translation of the ISR effector ATF4.[17,18] Thus, CC-90009 induced degradation of GSPT1 ultimately leads to accumulation of ATF4 plus its transcriptional targets CHOP and ATF3 with subsequent induction of apoptosis in leukemic blasts (Figure 2B).[19,20]

CC-90009 is a potent GSPT1 degrader with a degradation EC_{50} = 9 nM and Y_{min} = 49 or in other terms with a degradation maximum (D_{max}) = 51% when measured in a cellular degradation assay at 4 h.[15] When GSPT1 degradation was measured at 20 h, the EC_{50} remained the same, but the depth of degradation increased (Y_{min} = 12; D_{max} = 88). CC-90009 is selective in its degradation over other proteins (IKZF1/3 EC_{50} > 10 μM). Further assessment of CC-90009's selectivity by proteomic experiments with concentration range from 0.20 μM up to 3 μM with 4 or 6 h incubation shows GSPT1 is the only detectable protein degraded with greater than −1 log2 fold change (~75% degradation).[20]

CC-90009 demonstrated antiproliferative activity in over 80% of the human AML cancer cell lines tested, and when examined in primary patient AML blasts, exerted this effect through rapid induction of apoptosis. In ex vivo studies employing AML patient bone marrow samples, growth inhibition of leukemic cells was 2- to 5-fold greater than the inhibition of normal adult lymphocytes. In 9 of the first 10 patient samples examined, CC-90009 was highly active and had an average EC_{50} ~ 6 nM.[19] When an additional 30 patient samples were evaluated, CC-90009 retained activity in ~80% of the samples, consistent with the in vitro AML cell lines tested.

In Vivo Pharmacology. CC-90009 effectively reduced tumor cell content in femur bone marrow in an HL-60 xenograft model of AML. Treatment was initiated 6 weeks postinoculation with vehicle and CC-90009. Treatment groups were terminated either on Day 7 (following 5 consecutive days of 5 mg/kg BID CC-90009) or on Day 11 (following 10 consecutive days of 2.5 mg/kg BID CC-90009) post treatment initiation. The primary end point for the study was percentage of $hCD33^+/CD45^+$ cells in the bone marrow by FACS analysis. Treatment with 5 mg/kg CC-90009 BIDx5 resulted in a significant (p = 0.0013) 54.0% reduction of human CD33+/CD45+ tumor cells in the BM when compared to the vehicle control group. Treatment with 2.5 mg/kg CC-90009 BIDx10 resulted in a significant (p < 0.0001) 71.5% reduction of human $CD33^+/CD45^+$ tumor cells in the bone marrow when compared to the vehicle control group.

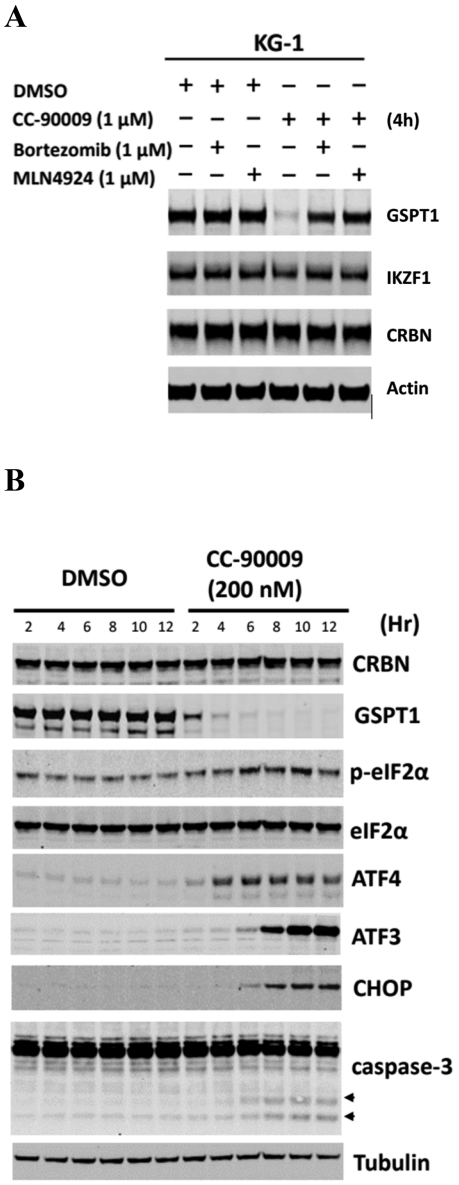

Figure 2. (A) Immunoblot analysis of KG1 cells treated with DMSO or CC-90009 for 4 h. Where indicated, cells were pretreated with bortezomib or MLN4924 for 30 min. (B) Immunoblot analysis of whole cell extracts of KG-1 cells. Cells were incubated with DMSO or 200 nM CC-90009 and lysed at the indicated time points. Arrows pointing to bands in the blot on the right designate the cleaved forms of caspase-3.[20]

https://dx.doi.org/10.1021/acs.jmedchem.0c01489
J. Med. Chem. 2021, 64, 1835−1843

Pharmacokinetics. Mouse pharmacokinetic studies were conducted in male CD-1 mice (n = 4). CC-90009 was dosed IV bolus to nonfasted mice at 2 mg/kg with a dose volume of 2 mL/kg in DMA/PEG400/5% dextrose in water (15:50:35). Samples were obtained via nonserial sampling due to the composite sampling design, and mean PK parameters are reported and listed in Table 4.

Table 4. Rodent and Monkey Pharmacokinetic Parameters Following IV Dosing for CC-90009

species	dose	CL (mL/min/kg)	V_{ss} (L/kg)	MRT (h)
mouse	IV dose (2 mg/kg)	67.9	1.00	0.24
rat	IV dose (2 mg/kg)	28.3 ± 0.7	2.2 ± 0.5	1.3 ± 0.3
monkey	IV dose (1 mg/kg)	6 ± 1	1.1 ± 0.1	4 ± 1

Rat pharmacokinetic studies were conducted in jugular vein cannulated male CD-IGS rats (n = 3). CC-90009 was dosed IV bolus to fed rats at 2 mg/kg with a dose volume of 2 mL/kg in DMA/PEG400/5% dextrose in water (15:50:35). The rat IV pharmacokinetic parameters are listed in Table 4.

A monkey PK study was conducted in male cynomolgus monkeys (n = 3). Data from the study are shown in Table 4. CC-90009 was dosed IV bolus to nonfasted monkeys at 1 mg/kg with a dose volume of 1 mL/kg in DMA/ethanol/PEG400/5% dextrose in water (5:10:40:45).

CC-90009 has a moderate to high clearance in the mouse, but a moderate to low clearance in rat and cynomolgus monkey, the preferred toxicology species. The metabolites of nonradiolabeled CC-90009 were investigated in hepatocytes from mouse, rat, monkey, and human. Additional metabolites were examined in vivo in the rat. Taken together, there were no unique human metabolites detected. Allometric scaling predicted a low human clearance of approximately 1.93 mL/min/kg and a volume of distribution of 1.48 L/kg.

In Vitro Safety. CC-90009 was determined to be modestly active (IC_{50} = 5.3 μM) against the human ether-à-go-go-related gene (hERG) ion channel. In a stand-alone nonpivotal in vivo cardiovascular safety pharmacology study in cynomolgus monkeys conducted with CC-90009, there were no CC-90009-related cardiovascular effects. CC-90009 (up to 2.5 μM) did not cause inhibition or induction of cytochrome P450 (CYP) enzymes in in vitro studies except for weak inhibition of CYP2C9 (41% at 2.5 μM) and CYP2C19 (IC_{50} = 1.53 μM). In addition, CC-90009 (up to 3 μM) did not inhibit P-gp, BCRP, MRP2, OAT1, OAT3, OATP1B1, OATP1B3, OCT2, or MATE2-K. CC-90009 was screened against a diverse panel of 255 kinases at 3 μM with no inhibition observed >20%. The selectivity of CC-90009 was explored further by evaluating its effect in binding assays for 80 different human receptors, ion channels, and transporters, and at a concentration of 10 μM, CC-90009 inhibited receptor binding ≥50% at only two receptors, $M_1(h)$ and $M_2(h)$.

Pharmaceutical Properties. CC-90009 appears as a white powder, and its crystallinity was confirmed by XRPD. Differential scanning calorimetry (DSC) showed a melting onset at 228 °C. The material used for clinical studies is an off-white material and is prepared as a racemic mixture of the R- and S-enantiomers as the single enantiomers demonstrated rapid in vitro and in vivo epimerization across multiple species. The formulation used for injection of CC-90009 is a lyophilized powder for reconstitution with sterile water to provide a solution that can yield a dose range from 0.6 to 20 mg.

Clinical Data. During the treatment period, CC-90009 is administered intravenously on days 1 to 5, days 1 to 7, or on days 1 to 3 and days 8 to 10 of each 28-day cycle for up to 4 cycles. Mean terminal half-life following the last day of dosing was estimated to be approximately 9.3 h. Upon 5 days of repeat

Scheme 1. Synthesis of CC-90009[a]

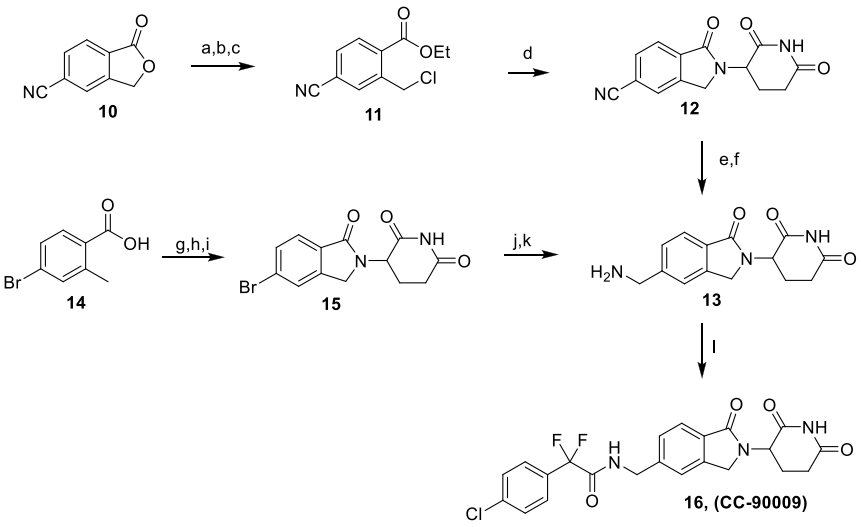

[a]Reagents and conditions: (a) 1 M NaOH, rt, 2 h, THF; (b) EtI, 80 °C, 1 h, DMF, 66% over 2 steps; (c) SO_2Cl_2, DCM, 0 °C, 16 h, 41%; (d) 3-aminopiperidine-2,6-dione·HCl, triethylamine, DMF, 70 °C, 16 h, 61%; (e) $NiCl_2$, $NaBH_4$, Boc_2O, NMP, rt, 15 h, 37%; (f) 4 M HCl-dioxane, rt, 2 h, 93%; (g) MeOH-H_2SO_4 (50-1), 65 °C, 18 h, 95%; (h) NBS, azo-isobutyronitrile, 85 °C, 18 h, ACN, 66%; (i) 3-aminopiperidine-2,6-dione.HCl, triethylamine, rt for 25 h, 44%; (j) 1,1′-bis(diphenylphosphino)ferrocene, ZnCN, ZnOAc, $Pd_2(dba)_3$, 120 °C for 20 h, 57%; (k) MsOH, Pd/C, DMA, 50 psi, 40 °C for 20 h, 40%, (l) 2-(4-chlorophenyl)-2,2-difluoroacetic acid, HATU, DIEA, DMF, 16 h, 86%.

https://dx.doi.org/10.1021/acs.jmedchem.0c01489
J. Med. Chem. 2021, 64, 1835−1843

dosing, a 1.2- to 2.7-fold accumulation of total systemic exposure was observed across dosing schedules. Across all doses and schedules, the geometric mean total clearance was 6.96 L/h, and volume of distribution was 61.69 L. In general, the exposures increased with dose in each dosing schedule. GSPT1 levels in $CD3^+$ T cells from individual patients treated with CC-90009 on D1−5 were measured by flow cytometry, and dose-dependent decreases in GSPT1 levels were observed in peripheral blood blasts and T cells. At a dose of 2.4 mg, 90% GSPT1 reduction was observed.[21]

Chemistry. The synthesis of CC-90009 (**16**) is outlined in Scheme 1. CC-90009 is made by coupling 2-(4-chlorophenyl)-2,2-difluoroacetic acid with the key intermediate **13**. The key benzylamine **13** can be derived in multiple ways, one of which begins with Fischer esterification of 4-bromo-2-methylbenzoic acid **14** followed by radical bromination of the tolyl methyl group.[22] Formation of the bicyclic lactam was accomplished using 3-aminopiperidine-2,6-dione as the nucleophile for bromide displacement followed by further condensation onto the ester to form lactam **15**. The requisite aminomethyl functionality was installed via palladium-mediated cyanide insertion to the aryl bromide with subsequent reduction to yield **13**. Alternatively, **13** could be synthesized starting from the lactone **10** by introduction of the amine functionality via nitrile reduction. This alternate starting point provides a route found to be convenient when used on larger scale and avoids the use of palladium near the end of the synthetic sequence.

CONCLUSION

During the course of SAR investigation, we discovered that replacement of the urea moiety in **3** with 2,2-difluoroacetamide could alter the profile of degraded proteins and demonstrated selectivity for GSPT1 over IKZF1/3. This optimized functionality held by CC-90009 led to the desired activity profile which maintained broad anti-AML activity but increased selectivity against a noncancer line like THLE-2, indicating a higher probability of achieving relevant therapeutic index. CC-90009 was shown to have an in vitro ADME and safety profile that supported additional studies in vivo and ultimately advanced into safety and efficacy studies in subjects with AML where a dose level of 2.4 mg resulted in 90% GSPT1 degradation.

The ability to design small molecules that catalytically orchestrate removal of "undruggable" proteins has tremendous potential to improve lives of countless patients when applied toward disease-driving proteins. An example where controlled protein homeostasis has revolutionized disease landscape can be gleaned from multiple myeloma, where proteasome inhibitors such as bortezomib and protein degraders such as lenalidomide have become the backbone therapy and dramatically increased five-year survival rates.[23] While lenalidomide was commercialized prior to understanding its degradation mechanism, CC-90009 in sharp contrast is the first CRBN-mediated protein degrader to enter clinical trials since the seminal discovery by Handa[24,25] linking CRBN to the immunomodulatory drugs.

In diversion from the IMiDs (lenalidomide, pomalidomide, and thalidomide) that degrade IKZF1/3, CC-90009 is the first small molecule molecular glue to be reported that selectively promotes the degradation of GSPT1. Our strategy employed phenotypic screening combined with E3-ligase directed chemical matter which helped uncover novel biology. This strategy may provide a roadmap for future advances we hope can be employed toward further addressing unmet medical need.

EXPERIMENTAL SECTION

General. Compounds were named using ChemDraw Ultra. All materials were obtained from commercial sources and used without further purification, unless otherwise noted. Chromatography solvents were HPLC grade and used as purchased. All air-sensitive reactions were carried out under a positive pressure of an inert nitrogen atmosphere. Chemical shifts (δ) are reported in ppm downfield of TMS and coupling constants (J) are given in Hz. Thin Layer Chromatography (TLC) analysis was performed on Whatman thin layer plates. The purity of final tested compounds was ≥95% as determined by HPLC using the following method: gradient (5−95% ACN + 0.075% formic acid in water +0.1% formic acid over 8 min, followed by 95% ACN + 0.075% formic acid for 2 min); flow rate 1 mL/min, column Phenomenex Luna 5 μ PFP(2) 100A (150 mm × 4.60 mm).

Synthesis. Compound **13** has been previously described in the literature.[26−29]

1-((2-(2,6-Dioxopiperidin-3-yl)-1-oxoisoindolin-5-yl)-methyl)-3-phenylurea (4). To a stirred mixture of 3-(5-(aminomethyl)-1-oxoisoindolin-2-yl)piperidine-2,6-dione methanesulfonate (0.37 g, 1.0 mmol) and phenylisocyanate (0.12 g, 1.0 mmol) in acetonitrile (10 mL) was added triethylamine (0.28 mL, 2.0 mmol) at room temperature under nitrogen. After 2 h, 1 N aq. HCl (10 mL) was added, and the solids were isolated by filtration and washed with water (20 mL). The solids were triturated in ethyl acetate (10 mL) for 18 h, then isolated by filtration, washed with ethyl acetate (40 mL), and dried under vacuum to give 1-((2-(2,6-dioxopiperidin-3-yl)-1-oxoisoindolin-5-yl)methyl)-3-phenylurea as a white solid (0.38 g, 0.97 mmol, 97% yield, HPLC purity >97%). ^{1}H NMR (300 MHz, DMSO-d_6) δ 10.97 (s, 1H), 8.61 (s, 1H), 7.69 (d, J = 7.8 Hz, 1H), 7.52 (s, 1H), 7.47−7.37 (m, 3H), 7.22 (t, J = 7.8 Hz, 2H), 6.89 (t, J = 7.3 Hz, 1H), 6.72 (t, J = 6.0 Hz, 1H), 5.10 (dd, J = 13.2, 5.1 Hz, 1H), 4.62−4.11 (m, 4H), 3.03−2.79 (m, 1H), 2.62−2.56 (m, 1H), 2.42−2.19 (m, 1H), 2.03−1.91 (m, 1H); MS (ESI) m/z 393.2 $[M + 1]^+$.

***N*-((2-(2,6-Dioxopiperidin-3-yl)-1-oxoisoindolin-5-yl)-methyl)-2-phenylacetamide (5).** To a solution of 2-phenylacetyl chloride (200 mg, 1.29 mmol) in acetonitrile (20 mL) was added 3-(5-(aminomethyl)-1-oxoisoindolin-2-yl)piperidine-2,6-dione methanesulfonate (434 mg, 1.17 mmol). The mixture was cooled to 0 °C, and triethylamine (264 mg, 2.6 mmol) was added dropwise. The reaction mixture was stirred at room temperature for 18 h. More 2-phenylacetyl chloride (200 mg) and more triethylamine (264 mg) was added and stirring continued for 5 h. To the mixture was added 1N aq. HCl (20 mL), dropwise. The resulting solids were collected by filtration, washed with ethyl acetate (30 mL), and dried in vacuo to give *N*-((2-(2,6-dioxopiperidin-3-yl)-1-oxoisoindolin-5-yl)methyl)-2-phenylacetamide (216 mg, 0.55 mmol, 47% yield, HPLC purity >98%). ^{1}H NMR (DMSO-d_6) δ 10.98 (s, 1H), 8.65 (t, J = 5.9 Hz, 1H), 7.66 (d, J = 7.7 Hz, 1H), 7.46−7.15 (m, 7H), 5.10 (dd, J = 5.1, 13.2 Hz, 1H), 4.50−4.19 (m, 4H), 3.50 (s, 2H), 3.01−2.82 (m, 1H), 2.63 (br. s, 1H), 2.39 (qd, J = 4.3, 13.2 Hz, 1H), 2.09−1.87 (m, 1H). MS (ESI) m/z 392.16 $[M + 1]^+$.

***N*-((2-(2,6-Dioxopiperidin-3-yl)-1-oxoisoindolin-5-yl)-methyl)benzamide (6).** To a stirred mixture of 3-(5-(aminomethyl)-1-oxoisoindolin-2-yl)piperidine-2,6-dione methanesulfonate (0.50 g, 1.80 mmol) and benzoyl chloride (0.25 g, 1.80 mmol) in acetonitrile (20 mL) was added triethylamine (0.51 mL, 3.60 mmol) at room temperature under nitrogen. After 1 h, 1N aq. HCl (20 mL) was added, and the mixture was stirred for 10 min. The product was isolated by filtration, washed with 1N aq. HCl (20 mL) and acetonitrile (20 mL), and dried overnight in vacuo to give *N*-((2-(2,6-dioxopiperidin-3-yl)-1-oxoisoindolin-5-yl)methyl)benzamide as a white solid (0.43 g, 1.14 mmol, 64% yield, HPLC purity >99%). ^{1}H NMR (400 DMSO-d_6) δ 10.99 (s, 1H), 9.16 (t, J = 5.9 Hz, 1H), 7.91 (d, J = 7.0 Hz, 2H), 7.70 (d, J = 7.7 Hz, 1H), 7.62−7.42 (m, 5H), 5.11 (dd, J = 5.0, 13.1 Hz, 1H), 4.60 (d, J = 5.9 Hz, 2H), 4.45 (d, J = 17.4 Hz, 1H), 4.31 (d, J = 17.4 Hz, 1H), 3.05−2.79 (m, 1H), 2.68−

https://dx.doi.org/10.1021/acs.jmedchem.0c01489
J. Med. Chem. 2021, 64, 1835−1843

2.53 (m, 1H), 2.47−2.27 (m, 1H), 2.06−1.93 (m, 1H); MS (ESI) *m/z* 378.15 $[M + 1]^+$.

***N*-((2-(2,6-Dioxopiperidin-3-yl)-1-oxoisoindolin-5-yl) methyl)-2-oxo-2-phenylacetamide (7).** *Step A.* To a stirred solution of 2-(2,6-dioxopiperidin-3-yl)-1-oxoisoindoline-5-carbonitrile (10 g, 37.13 mmol) in dimethylacetamide (320 mL) were added methanesulfonic acid (2.6 mL, 40.85 mmol) and 10% dry palladium on carbon (4 g) and stirred at hydrogen pressure under 50 psi at 40 °C for 20 h in a hydrogen vessel. The reaction mixture was filtered through Celite and washed with water (100 mL). The filtrate was concentrated under reduced pressure, and the resultant residue was triturated with 1% methanol in dichloromethane to give 3-(5-(aminomethyl)-1-oxoisoindolin-2-yl)piperidine-2,6-dione methanesulfonate (5.6 g, 15.17 mmol, 40% yield) as an off-white solid. MS (ESI) *m/z* 272.0 $[M - 1]^+$.

Step B. To a stirred cold (0 °C) solution of 3-(5-(aminomethyl)-1-oxoisoindolin-2-yl)piperidine-2,6-dione methanesulfonate (300 mg, 0.813 mmol) in *N*,*N*-dimethylacetamide (10 mL) was added 2-oxo-2-phenylacetic acid (122 mg, 0.813 mmol) followed by *N*,*N*-diisopropylethylamine (0.5 mL, 2.43 mmol) and 1-[bis-(dimethylamino)methylene]-1*H*-1,2,3-triazolo[4,5-*b*]pyridinium 3-oxid hexafluorophosphate (402 mg, 1.056 mmol) and stirred at room temperature for 16 h. The reaction mixture was diluted with water (100 mL), the solid obtained was filtered, washed with diethyl ether (20 mL), dried and purified by column chromatography (100−200 silica) using 3% methanol in dichloromethane as eluent to give (55 mg, 0.135 mmol, 17% yield, HPLC purity >97%) as an off white solid. ^{1}H NMR (400 MHz, DMSO-d_6) δ (ppm) 10.98 (s, 1H), 9.56 (d, *J* = 6.2 Hz, 1H), 8.08−7.86 (m, 2H), 7.80−7.66 (m, 2H), 7.63−7.55 (m, 3H), 7.49 (d, *J* = 7.8 Hz, 1H), 5.12 (dd, *J* = 13.3, 5.1 Hz, 1H), 4.58 (d, *J* = 6.0 Hz, 2H), 4.48 (d, *J* = 17.4 Hz, 1H), 4.33 (d, *J* = 17.3 Hz, 1H), 2.99−2.83 (m, 1H), 2.73 (s, 1H), 2.63 (s, 1H), 2.27 (s, 1H); MS (ESI) *m/z* 406.14 $[M + 1]^+$.

***N*-((2-(2,6-Dioxopiperidin-3-yl)-1-oxoisoindolin-5-yl)-methyl)-2-methyl-2-phenylpropanamide (8).** To a cooled (0 °C) solution of 3-(5-(aminomethyl)-1-oxoisoindolin-2-yl)piperidine-2,6-dione hydrochloride (200 mg, 0.65 mmol) in *N*,*N*-dimethylacetamide (4 mL) were added 2-methyl-2-phenylpropanoic acid (106 mg, 0.65 mmol) and 1-[bis(dimethylamino)methylene]-1*H*-1,2,3-triazolo[4,5-*b*]pyridinium 3-oxid hexafluorophosphate (369 mg, 0.97 mmol) followed by diisopropylethylamine (0.34 mL, 1.94 mmol) and stirred at room temperature for 16 h. The volatiles were removed under reduced pressure, and the resultant residue was poured into water (10 mL). The precipitated solid was filtered and purified by Reveleris C-18 reversed phase column chromatography (55−60% acetonitrile/0.1% aqueous formic acid) to afford *N*-((2-(2,6-dioxopiperidin-3-yl)-1-oxoisoindolin-5-yl)methyl)-2-methyl-2-phenylpropanamide (105 mg, 0.25 mmol, 39% yield, HPLC purity >99%) as an off-white solid. ^{1}H NMR (400 MHz, DMSO-d_6) δ 10.98 (s, 1H), 8.02 (t, *J* = 6.0 Hz, 1H), 7.61 (d, *J* = 8.0 Hz, 1H), 7.33−7.21 (m, 7H), 5.10 (dd, *J* = 14.0, 5.6 Hz, 1H), 4.48 (d, *J* = 16.8 Hz, 1H), 4.33 (d, *J* = 5.6 Hz, 2H), 4.24 (d, *J* = 17.2 Hz, 1H), 2.96−2.87 (m, 1H), 2.62−2.58 (m, 1H), 2.44−2.39 (m, 1H), 2.38−1.97 (m, 1H), 1.49 (s, 6H); MS (ESI) *m/z* 420.19 $[M + 1]^+$.

***N*-((2-(2,6-Dioxopiperidin-3-yl)- l-oxoisoindolin-5-yl)-methyl)-2,2-.** *Difluoro-2-phenylacetamide (**9**).* 3-(5-(Aminomethyl)-1 -oxoisoindolin-2-yl)piperidine-2,6-dione, mesylic acid (0.050 g, 0.135 mmol), was placed in a vial with N,N-dimethylformamide (1.0 mL), 2,2-difluoro-2-phenylacetic acid (0.023 g, 0.135 mmol), diisopropylethylamine (0.071 mL, 0.406 mmol), and 1-[bis-(dimethylamino)methylene]-1*H*-1,2,3-triazolo[4,5-*b*]pyridinium 3-oxide hexafluorophosphate (0.057 g, 0.149 mmol). The reaction mixture was stirred at room temperature for 18 h. The reaction mixture was taken up in dimethyl sulfoxide and purified using reverse-phase semi preparatory HPLC (5−100% acetonitrile + 0.1% formic acid in water + 0.1% formic acid over 20 min). Fractions containing desired product were combined, and volatile organics were removed under reduced pressure to give *N*-((2-(2,6-dioxopiperidin-3-yl)-l-oxoisoindolin-5-yl)methyl)-2,2-difluoro-2-phenylacetamide (0.039 g, 0.091 mmol, 67.4% yield, HPLC purity >99%) as a white solid. ^{1}H NMR (400 MHz, DMSO-d_6) δ 11.00 (s, 1H), 9.67 (t, *J* = 6.25 Hz, 1H), 7.67 (d, *J* = 7.81 Hz, 1H), 7.50−7.62 (m, 5H), 7.34- 7.42 (m, 2H), 5.11 (dd, *J* = 5.08, 13.28 Hz, 1H), 4.38−4.47 (m, 3H), 4.24−4.31 (m,1H), 2.86−2.97 (m, 1H), 2.55−2.64 (m, 1H), 2.32−2.45 (m, 1H), 1.99 (dtd, *J* = 2.34, 5.25, 12.55 Hz, 1H). MS (ESI) *m/z* 428.14 $[M+l]^+$.

*2-(4-Chlorophenyl)-N-((2-(2,6-dioxopiperidin-3-yl)-l-oxoisoindolin-5-yl)methyl)-2,2-difluoroacetamide (**16**).* To 3-(5-(aminomethyl)-1 -oxoisoindolin-2- yl)piperidine-2,6-dione methanesulfonate **13** (15.0 g, 40.6 mmol) in N,N-dimethylformamide (100 mL) was added 1-[bis(dimethylamino)methylene]-1*H*-1,2,3-triazolo[4,5-*b*]-pyridinium 3-oxid hexafluorophosphate (16.9 g, 44.7 mmol) and 2-(4-chlorophenyl)-2,2-difluoroacetic acid (8.4 g, 40.6 mmol) followed by diisopropylethylamine (21.3 mL, 122 mmol). The mixture was allowed to stir at 25 °C for 24 h and then partitioned between 1500 mL of water and 1500 mL of EtOAc. The organic layer was washed with saturated sodium bicarbonate solution (2 × 500 mL), 1 N HCl solution (2 × 500 mL), and then brine (2 × 300 mL). The organic layer was then concentrated under reduced pressure to afford a white solid which was slurried in water for 30 min and collected by vacuum filtration. The solids were digested with isopropanol and refluxed for 1 h. After cooling to room temperature, the solids were collected by vacuum filtration to afford 2-(4-chlorophenyl)-*N*-((2-(2,6-dioxopiperidin-3-yl)-loxoisoindolin-5-yl)methyl)-2,2-difluoroacetamide (16.1 g, 34.8 mmol, 85.7% yield, HPLC purity >99%) as a white solid. ^{1}H NMR (500 MHz, DMSO-d6) δ ppm 10.98 (s, 1H), 9.68 (t, *J* = 6.15 Hz, 1H), 7.69 (d, *J* = 7.88 Hz, 1H), 7.58−7.66 (m, 4H), 7.33−7.44 (m, 2H), 5.11 (dd, *J* = 13.24, 5.04 Hz, 1H), 4.39−4.50 (m, 3H), 4.24−4.35 (m, 1H), 2.85−2.98 (m, 1H), 2.61 (dd, *J* = 15.29, 2.05 Hz, 1H), 2.39 (dd, *J* = 12.93, 4.73 Hz, 1H), 1.95−2.07 (m, 1H). MS (ESI) *m/z* 462.2 $[M+l]^+$.

ePL Degradation Assay. DF15 multiple myeloma cells stably expressing ePL-tagged GSPT1 were generated via lentiviral infection with pLOC-ePL-GSPT1. Cells were dispensed into a 384-well plate (Corning #3712) prespotted with compound. Compounds were dispensed by an acoustic dispenser (ATS Acoustic Transfer System from EDC Biosystems) into a 384-well in a 10 pt dose response curve using 3-fold dilutions starting at 10 μM and going down to 0.0005 μM in DMSO. A DMSO control is added to the assay. Twenty-five microliters of media (RPMI-1640 + 10% Heat Inactivated FBS + 25 mM Hepes+1 mM Na Pyruvate + 1× NEAA + 0.1% Pluronic F-68 + 1× Pen Strep Glutamine) containing 5000 cells was dispensed per well. Assay plates were incubated at 37 °C with 5% CO_2 for 4 h. After incubation, 25 μL of the InCELL Hunter Detection Reagent Working Solution (DiscoverX, cat #96-0002, Fremont, CA) was added to each well and incubated at room temperature for 30 min protected from light. After 30 min, luminescence was read on a PHERAstar luminometer (Cary, NC).

To determine EC_{50} values for GSPT1 degradation, a four-parameter logistic model (sigmoidal dose−response model) (FIT= $(A + ((B - A)/1 + ((C/x)D)))$, where *C* is the inflection point (EC_{50}), *D* is the correlation coefficient, and *A* and *B* are the low and high limits of the fit, respectively) was used to determine the compound's EC_{50} value, which is the half-maximum effective concentration. The minimum *Y* is reference to the *Y* constant. In the GSPT1 degradation assay, we used compound **3** as the control with a *Y* constant = 0. The maximum limit is the *Y* max DMSO control. All percent of control GSPT1 degradation curves were processed and evaluated using Activity Base (IDBS). The maximum limit is the *Y* max DMSO control. All percent of control GSPT1 degradation curves were processed and evaluated using Activity Base (IDBS).

Cell Culture. Acute myeloid leukemia cell lines KG-1, Kasumi-1, U937, MOLM-13, HL-60, and MV-4-11 were purchased from American Tissue Culture Collection (ATCC). NB-4, HNT-34, OCI-AML2, and OCI-AML3 cell lines were purchased from Deutsche Sammlung von Mikroorganismen and Zellkulturen GmbH. 293FT *CRBN*−/−, MOLM-13 *CRBN*−/−, and OCI-AML2 *CRBN*−/− cell lines were described previously. KG-1, Kasumi-1, U937, MOLM-13, NB-4, and HNT-34 cell lines were maintained in Roswell Park

https://dx.doi.org/10.1021/acs.jmedchem.0c01489
J. Med. Chem. 2021, 64, 1835−1843

Memorial Institute (RPMI) 1640 tissue culture medium (Invitrogen) supplemented with 10% FBS, 1× sodium pyruvate, 1× nonessential amino acids, 100 U/mL penicillin, and 100 μg/mL streptomycin. HL-60 and MV-4-11 cell lines were maintained in Iscove's modified Dulbecco's medium (IMDM; Invitrogen) supplemented with 10% FBS, 1× sodium pyruvate, 1× nonessential amino acids, 100 U/mL penicillin, and 100 μg/mL streptomycin. OCI-AML2 and OCI-AML3 cell lines were maintained in minimal essential medium (MEM; Invitrogen) supplemented with 10% FBS, 1× sodium pyruvate, 1× nonessential amino acid, 100 U/mL penicillin, and 100 μg/mL streptomycin.

Cell Proliferation Assay. Human cancer cell lines cultured in the growth medium recommended by the vendor were seeded into black 384-well plates containing DMSO or test compounds. The seeding density of each cell line was optimized to allow for cell growth in the linear range during a 3-day culture period. To test the compound effect on cell proliferation in AML cell lines, 5000 to 10000 cells per well in 200 μL complete culture media were seeded into black 96-well plates containing DMSO or test compounds. After 72 h, cell proliferation was assessed using CTG according to the manufacturer's instructions. The growth inhibitory IC_{50} values of CC-90009 were determined using ActivityBase (IDBS).

Cell Apoptosis Assay. The ability of CC-90009 to induce apoptosis was assessed in selected AML cell lines at the time points and compound concentrations indicated. For Annexin V/7AAD readout by flow cytometry, AML cell lines were plated into flat bottom 96-well plates (BD Falcon) at a seeding density of 0.1−0.3 × 106 cells per mL in 200 μL complete media. CC-90009 was dispensed onto the plates, and the cells were incubated for 24−48 h. At the end of the incubation period, 100 μL of cells were transferred into a 96-well U-bottom plate (BD Falcon), centrifuged at 1200 rpm for 5 min, and the media was removed. Then, 2.5 μL of Annexin V-AF647 (Biolegend) and 5 μL 7AAD (Biolegend) were diluted into 100 μL of 1× Annexin binding buffer (BD Biosciences). Fifteen minutes after addition of 100 μL of Annexin V/7AAD buffer into each well, cells were analyzed using the Attune Flow Cytometer (Invitrogen). The apoptosis induction curve was processed and graphed using GraphPad Prism Version 7 ($P < 0.05$, unpaired two-sided t test, is considered as significant).

Proteomics. KG1 cells were treated with DMSO or 100 nM CC-90009 for 4 h. All treatments were performed with four replicates and protein lysates were digested with trypsin, labeled by isobaric tandem-mass-tags (TMT), fractionated, and analyzed using an Orbitrap Fusion Lumos mass spectrometer at IQ Proteomics (Cambridge, MA). Peptide to protein mapping, protein identification, and quantification of relative protein abundance with statistical analyses were performed at Celgene using custom software. 7957 human proteins were unambiguously quantified by at least one peptide in at least one of the MS runs. Proteins were defined by the Uniprot identifier, with some represented by more than one isoform.

Immunoblot Analysis. Cells were washed in ice-cold 1× PBS twice before harvest in Buffer A [50 mM Tris·Cl (pH 7.6), 150 mM NaCl, 1% Triton X-100, 1 mM EDTA, 1 mM EGTA, 1 mM β-glycerophosphate, 2.5 mM sodium pyrophosphate, 1 mM Na3VO4, 1 μg/mL leupeptin, one tablet of Complete ULTRA protease inhibitor cocktail (Roche), and one tablet of PhosSTOP phosphatase inhibitor cocktail (Roche)]. Whole cell extracts were collected after centrifugation at top speed for 10 min and total protein was quantified using Bradford Reagent (Bio-Rad) according to the manufacturer's instructions. Then, 10−20 μg of total protein per sample were resolved by SDS-PAGE gel electrophoresis, transferred onto a nitrocellulose membrane using the Turboblot system (Bio-Rad), and probed with the indicated primary antibodies. Bound antibodies were detected with IRDye-680 or -800 conjugated secondary antibodies using a LI-COR scanner.

ANIMAL USE

All animal studies were performed under protocols approved by the Celgene Institutional Animal Care and Use Committee (IACUC). Animals were acclimatized to the animal housing facility for a period of seven days prior to the beginning of the experiment.

ASSOCIATED CONTENT

Supporting Information

The Supporting Information is available free of charge at https://pubs.acs.org/doi/10.1021/acs.jmedchem.0c01489.

Biological data and molecular formula strings (CSV)
HPLC traces (PDF)

AUTHOR INFORMATION

Corresponding Author

Joshua D. Hansen − *Bristol Myers Squibb, San Diego, California 92121, United States*; orcid.org/0000-0002-4881-5247; Phone: 858-795-4910; Email: joshua.hansen@bms.com

Authors

Matthew Correa − *Bristol Myers Squibb, San Diego, California 92121, United States*
Matt Alexander − *Bristol Myers Squibb, San Diego, California 92121, United States*
Mark Nagy − *Bristol Myers Squibb, San Diego, California 92121, United States*
Dehua Huang − *Bristol Myers Squibb, San Diego, California 92121, United States*
John Sapienza − *Bristol Myers Squibb, San Diego, California 92121, United States*
Gang Lu − *Bristol Myers Squibb, San Diego, California 92121, United States*
Laurie A. LeBrun − *Bristol Myers Squibb, San Diego, California 92121, United States*
Brian E. Cathers − *Bristol Myers Squibb, San Diego, California 92121, United States*
Weihong Zhang − *Bristol Myers Squibb, Summit, New Jersey 07901, United States*
Yang Tang − *Bristol Myers Squibb, San Diego, California 92121, United States*
Massimo Ammirante − *Bristol Myers Squibb, San Diego, California 92121, United States*
Rama K. Narla − *Bristol Myers Squibb, San Diego, California 92121, United States*
Joseph R. Piccotti − *Bristol Myers Squibb, San Diego, California 92121, United States*
Michael Pourdehnad − *Bristol Myers Squibb, San Francisco, California 94158, United States*
Antonia Lopez-Girona − *Bristol Myers Squibb, San Diego, California 92121, United States*

Complete contact information is available at: https://pubs.acs.org/10.1021/acs.jmedchem.0c01489

Notes

The authors declare no competing financial interest.

ACKNOWLEDGMENTS

We acknowledge Thomas Daniel, Greg Reyes, Neil Raheja, and Katerina Leftheris for their encouraging support of this work. We also acknowledge our compound management and analytical groups for technical assistance and sample processing as well as thank Dr. Ravi Kumar and his team at GVK Bio for synthetic support.

ABBREVIATIONS

CELMoD, Cereblon E3 Ligase Modulating Drug; CRBN, Cereblon; CUL4, cullin-4 protein; DDB1, damaged DNA-binding protein 1; RBX1, RING box-domain protein; GSPT1, G1 to S phase transition 1; DUB, deubiquitinating enzyme; eRF3a, eukaryotic release factor 3a; NBS, *N*-bromosuccinimide; ACN, acetonitrile; HCl, hydrochloric acid; DMA, dimethylacetamide; DMF, dimethylformamide; TLC, thin layer chromatography; HPLC, high performance liquid chromatography

REFERENCES

(1) Stein, E. M.; Tallman, M. S. Emerging Therapeutic Drugs for AML. *Blood* **2016**, *127*, 71−78.

(2) American Cancer Society, Cancer Statistic Center Page. https://www.cancer.org/cancer/acute-myeloid-leukemia/about/key-statistics.html (accessed June 1, 2020).

(3) Meyers, J.; Yu, Y.; Kaye, J. A.; Davis, K. L. Medicare Free-for-Service Enrollees with Primary Acute Myeloid Leukemia: An Analysis of Treatment Patterns, Survival, and Healthcare Resource Utilization and Costs. *Appl. Health Econ Health Policy* **2013**, *11*, 275−286.

(4) DiNardo, C. D.; Jonas, B. A.; Pullarkat, V.; Thirman, M. J.; Garcia, J. S.; Wei, A. H.; Konopleva, M.; Döhner, H.; Letai, A.; Fenaux, P.; Koller, E.; Havelange, V. Azacitidine and Venetoclax in Previously Untreated Acute Myeloid. *N. Engl. J. Med.* **2020**, *383*, 617−629.

(5) Deshaies, R. J. Multispecific Drugs Herald a New Era of Biopharmaceutical Innovation. *Nature* **2020**, *580*, 329−338.

(6) Sun, X.; Gao, H.; Yang, Y.; He, M.; Wu, Y.; Song, Y.; Tong, Y.; Rao, Y. PROTACs: Great Opportunities for Academia and Industry. *Sig. Transduct. Target. Ther.* **2019**, *64*, 1−33.

(7) Chamberlain, P.; D'Agostino, L.; Ellis, M. J.; Hansen, J. D.; Matyskiela, M.; McDonald, J. J.; Riggs, J. R.; Hamann, L. G. Evolution of Cereblon-Mediated Protein Degradation as a Therapeutic Modality. *ACS Med. Chem. Lett.* **2019**, *10* (12), 1592−1602.

(8) U.S. National Library of Medicine. Clinical Trials.gov. https://clinicaltrials.gov/ct2/show/NCT04428788, https://clinicaltrials.gov/ct2/show/NCT03888612, https://clinicaltrials.gov/ct2/show/NCT04072952; (accessed December 20, 2020).

(9) U.S. National Library of Medicine. Clinical Trials.gov. https://clinicaltrials.gov/ct2/show/NCT02848001?term=CC-90009&draw=2&rank=2, https://clinicaltrials.gov/ct2/show/NCT03374085, https://clinicaltrials.gov/ct2/show/NCT03930953, https://clinicaltrials.gov/ct2/show/NCT03891953, (accessed December 20, 2020).

(10) Ito, T.; Ando, H.; Suzuki, T.; Ogura, T.; Hotta, K.; Imamura, Y.; Yamaguchi, Y.; Handa, H. Identification of a Primary Target of Thalidomide Teratogenicity. *Science* **2010**, *327*, 1345−1350.

(11) Kronke, J.; Udeshi, N. D.; Narla, A.; Grauman, P.; Hurst, S. N.; McConkey, M.; Svinkina, T.; Heckl, D.; Comer, E.; Li, X.; Ciarlo, C.; Hartman, E.; Munshi, N.; Schenone, M.; Schreiber, S. L.; Carr, S. A.; Ebert, B. L. Lenalidomide Causes Selective Degradation of IKZF1 and IKZF3 in Multiple Myeloma Cells. *Science* **2014**, *343*, 301−305.

(12) Lu, G.; Middleton, R. E.; Sun, H.; Naniong, M.; Ott, C. J.; Mitsiades, C. S.; Wong, K. K.; Bradner, J. E.; Kaelin, W. G., Jr The Myeloma Drug Lenalidomide Promotes the Cereblon-Dependent Destruction of Ikaros Proteins. *Science* **2014**, *343*, 305−309.

(13) Moffat, J.; Vincent, F.; Lee, J.; Eder, J.; Prunotto, M. Opportunities and Challenges in Phenotypic Drug Discovery: An Industry Perspective. *Nat. Rev. Drug Discovery* **2017**, *16*, 531−543.

(14) Handschuh, L. Not Only Mutations Matter: Molecular Picture of Acute Myeloid Leukemia Emerging from Transcriptome Studies. *J. Oncol.* **2019**, *2019*, 7239206.

(15) Hansen, J. D.; Condroski, K.; Correa, M.; Muller, G.; Man, H. W.; Ruchelman, A.; Zhang, W.; Vocanson, F.; Crea, T.; Liu, W.; Lu, G.; Baculi, F.; LeBrun, L.; Mahmoudi, A.; Carmel, G.; Hickman, M.; Lu, C. C. Protein Degradation via CRL4CRBN Ubiquitin Ligase: Discovery and Structure-Activity Relationships of Novel Glutarimide Analogs that Promote Degradation of Aiolos and/or GSPT1. *J. Med. Chem.* **2018**, *61* (2), 492−503.

(16) Shah, F.; Louise-May, S.; Greene, N. Chemotypes Sensitivity and Predictivity of In Vivo Outcomes for Cytotoxic Assays in THLE and HepG2. *Bioorg. Med. Chem. Lett.* **2014**, *24*, 2753−2757.

(17) Baird, T. D.; Wek, R. C. Eukaryotic Initiation Factor 2 Phosphorylation and Translational Control in Metabolism. *Adv. Nutr.* **2012**, *3*, 307−321.

(18) Donnelly, N.; Gorman, A. M.; Gupta, S.; Samali, A. The eIF2 Alpha Kinases: Their Structures and Functions. *Cell. Mol. Life Sci.* **2013**, *70*, 3493−3511.

(19) Lu, G.; Surka, C.; Lu, C. C.; Jang, I. S.; Wang, K.; Rolfe, M. Elucidating the Mechanism of Action of CC-90009, a Novel Cereblon E3 Ligase Modulator, in AML via Genome-Wide CRISPR Screen. *Blood* **2019**, *134*, 405.

(20) Surka, C.; Jin, L.; Mbong, N.; Lu, C.; Jang, I.; Rychak, E.; Mendy, D.; Clayton, T.; Tindall, E. A.; Hsu, C.; Fontanillo, C.; Tran, E.; Contreras, A.; Ng, S. W.; Matyskiela, M. E.; Wang, K.; Chamberlain, P. P.; Cathers, B.; Carmichael, J.; Hansen, J. D.; Wang, J. C.Y.; Minden, M. D.; Fan, J.; Pierce, D. W.; Pourdehnad, M.; Rolfe, M.; Lopez-Girona, A.; Dick, J. E.; Lu, G. CC-90009, a Novel Cereblon E3 Ligase Modulator Targets Acute Myeloid Leukemia Blasts and Leukemia Stem Cells. *Blood* **2021**, *137*, 661.

(21) Fan, J.; Wang, H.; Couto, S.; Yao, T. W.; Uy, G. L.; Zeidan, A. M.; Minden, M. D.; Montesinos, P.; DeAngelo, D. J.; Altman, J. K.; Koprivnikar, J.; Vyas, P.; Fløisand, Y.; Vidriales, M. B.; Gjertsen, B. T.; Buchholz, T. J.; Pourdehnad, M.; Pierce, D. W. Pharmacodynamic Responses to CC-90009, a Novel Cereblon E3 Ligase Modulator, in a Phase I Dose-Escalation Study in Relapsed or Refractory Acute Myeloid Leukemia (R/R AML). *Blood* **2019**, *134*, 2547.

(22) Muller, G. W.; Ruchelman, A. L. 5-Substituted Isoindoline Compounds for the Use in Cancer. WO 2010053732, 2010.

(23) Thorsteinsdottir, S.; Dickman, P.; Landgren, O.; Blimark, O.; Hultcrantz, M.; Turesson, I.; Bjorkholm, M.; Kristinsson, S. Dramatically Improved Survival in Multiple Myeloma Patients in the Recent Decade: Results from a Swedish Population-Based Study. *Haematologica* **2018**, *103*, 412−415.

(24) Ito, T.; Ando, H.; Suzuki, T.; Ogura, T.; Hotta, K.; Imamura, Y.; Yamaguchi, Y.; Handa, H. Identification of a Primary Target of Thalidomide Teratogenicity. *Science* **2010**, *327*, 1345−1350.

(25) Lopez-Girona, A.; Mendy, D.; Ito, T.; Miller, K.; Gandhi, A.; Kang, J.; Karasawa, S.; Carmel, G.; Jackson, P.; Abbasian, M.; Mahmoudi, A.; Cathers, B.; Rychak, E.; Gaidarova, S.; Chen, R.; Schafer, P.; Handa, H.; Daniel, T. O.; Evans, J.; Chopra, R. Cereblon is a Direct Protein Target for Immunomodulatory and Antiproliferative Activities of Lenalidomide and Pomalidomide. *Leukemia* **2012**, *26*, 2326−2335.

(26) Muller, G. W.; Ruchelman, A. L.; Chen, R. 5-Substituted Isoindoline Compounds. US 20090142297, 2009.

(27) Muller, G. W.; Ruchelman, A. L.; Chen, R. 5-Substituted Isoindoline Compounds. WO 2008027542, 2008.

(28) Hansen, J.; Zhang, W.; Preparation of Isotopologues of 2-(4-chlorophenyl)-N-((2-(2,6-dioxopiperidin-3-yl)-1-oxoisoindolin-5-yl)-methyl)-2,2-difluoroacetamide as Antitumor Agents. WO 2019136016, 2019.

(29) Hansen, J.; Correa, M. D.; Raheja, R.; Lopez-Girona, A.; Man, H.-W.; Muller, G. W.; Macbeth, K.; Cathers, B.; Pourdehnad, M. Antiproliferative Compounds and Methods of Use Thereof. WO 2016007848, 2016.

https://dx.doi.org/10.1021/acs.jmedchem.0c01489
J. Med. Chem. 2021, 64, 1835−1843